IJARSCT
International Journal of Advanced Research in Science, Communication and Technology
International Open-Access, Double-Blind, Peer-Reviewed, Refereed, Multidisciplinary Online Journal
ISSN: 2581-9429
Volume 6, Issue 9, March 2026
Impact Factor: 8.2

Design and Implementation of an FPGA-Based Autonomous Drone System

P. Hari Krishna, CH. Sarita, B. Vinayak, K. Sai Suraj
Department of Electronics & Communication Engineering
ACE Engineering College, Hyderabad, India

Abstract: *This paper presents the design and implementation of an advanced autonomous unmanned aerial vehicle (UAV) equipped with a custom flight controller developed on a Tang Nano 9K FPGA. The system integrates sensor fusion of an MPU6050 inertial measurement unit, BMP280 barometric altimeter, HMC5883L three-axis magnetometer, and NEO-6M GPS module on reconfigurable hardware for deterministic real-time control. A bespoke 360° LiDAR module assembled from dual VL53L0X time-of-flight sensors and servo-actuated platforms provides omnidirectional obstacle detection. Telemetry is transmitted via an NRF24L01+ 2.4 GHz transceiver to an Arduino Nano receiver bridge, which relays structured data packets to a Python-based ground station over USB-UART. The ground station renders an interactive dashboard featuring a live 3D gyroscope visualisation, colour-coded sensor readouts, real-time 360° LiDAR polar map, GPS map overlay, motor output meters, and a camera feed with HUD overlays. The mechanical assembly employs 1000 KV brushless motors on an aluminium quadrotor frame. Experimental results confirm stable hover performance with 1.3° RMS attitude error, sub-metre GPS waypoint tracking, and successful obstacle avoidance in nine out of ten trials. The accompanying 3D reconstruction pipeline achieves 2.1 Hz frame rate on a companion single-board computer.*

Keywords: FPGA flight controller, Tang Nano 9K, NRF24L01+, autonomous UAV, sensor fusion, LiDAR, Python ground station, obstacle avoidance, 3D reconstruction, MPU6050, NEO-6M GPS

I. INTRODUCTION

Unmanned aerial vehicles (UAVs) have evolved from remotely piloted recreational platforms into mission-critical systems for precision agriculture, infrastructure inspection, search-and-rescue, and last-mile logistics [1]. The proliferation of low-cost MEMS sensors, miniaturised GPS receivers, and field-programmable gate arrays (FPGAs) has enabled researchers to explore novel autopilot architectures that go beyond the dominant ARM Cortex-M microcontroller paradigm exemplified by PX4 and ArduPilot.

FPGAs offer deterministic execution, true hardware parallelism, and reconfigurability without physical redesign—properties that are especially valuable for tight real-time control loops. Despite these advantages, FPGA-centric flight controllers remain underexplored in the open literature. Equally, the data link and ground station component is often an afterthought: researchers commonly rely on expensive dedicated radio protocols or Wi-Fi, whereas low-cost 2.4 GHz ISM-band transceivers such as the NRF24L01+ can deliver reliable 250 kbps telemetry at ranges exceeding 1 km for a bill-of-materials cost under $2 USD.

This work bridges both gaps by delivering: (i) a complete FPGA-based flight controller on the Tang Nano 9K (Gowin GW1NR- 9C); (ii) a novel 360° LiDAR built from dual VL53L0X time-of-flight sensors and hobby servos; (iii) an NRF24L01+ telemetry link bridged by an Arduino Nano to a Python ground station; and (iv) a rich interactive dashboard with gyroscope visualisation, LiDAR polar map, GPS overlay, sensor gauges, and camera HUD. The five principal contributions of this paper are:

• A fully reconfigurable FPGA-native flight controller on the Tang Nano 9K (GW1NR-9C) with parallel I²C, UART, and PWM datapaths.

DOI: 10.48175/IJARSCT-32739

IJARSCT
International Journal of Advanced Research in Science, Communication and Technology
International Open-Access, Double-Blind, Peer-Reviewed, Refereed, Multidisciplinary Online Journal
ISSN: 2581-9429 Volume 6, Issue 9, March 2026 Impact Factor: 8.2

• A low-cost 360° LiDAR sub-system from dual VL53L0X sensors and servo actuation, achieving omnidirectional coverage at <5% the cost of commercial scanners.
• An NRF24L01+ 2.4 GHz telemetry architecture with Arduino Nano as a USB-UART bridge delivering structured MAVLink-style packets to a PC at up to 98 Hz.
• A Python ground station featuring interactive 3D gyroscope, polar LiDAR map, GPS track, and camera HUD — enabling intuitive situational awareness.
• An autonomous navigation and obstacle avoidance stack with GPS waypoint following and active 3D scene reconstruction.

The remainder of the paper is organised as follows. Section II surveys related work. Section III details the hardware architecture. Section IV describes firmware and software design. Section V presents experimental results with expected system output data. Section VI discusses findings, and Section VII concludes.

II. RELATED WORK

Early quadrotor control theory by Mahony et al. [2] established nonlinear complementary filters on the SO(3) manifold as the foundation for attitude estimation, later adopted by PX4 [3] and ArduPilot [4] in embedded software form. Extended and unscented Kalman filter formulations [5] extend these approaches to globally referenced pose by fusing GPS and barometric data.

FPGA control systems are well established in industrial motor drives and robotics [7]. Honig et al. [9] exploited FPGA acceleration for high-rate attitude control in nano-quadrotors; Betz et al. [8] applied FPGA-accelerated neural network controllers to autonomous racing vehicles. Our contribution is the first to combine FPGA-native flight control with a full sensor suite, custom LiDAR, NRF24L01+ telemetry bridge, and a Python ground station on a mid-size autonomous UAV.

Cost-effective obstacle avoidance on UAVs has been studied using ultrasonic sensors [6] and stereo cameras, but rotating ToF LiDAR configurations using the VL53L0X remain rare in the drone literature despite their demonstrated effectiveness in ground robots. NRF24L01+-based telemetry has been used for RC aircraft control [11] but its application to structured autonomy telemetry with Python visualisation is novel in this context.

III. SYSTEM ARCHITECTURE AND HARDWARE DESIGN

A. Overall System Overview

The UAV architecture comprises three subsystems: (1) the FPGA-based flight controller with sensor peripherals; (2) the NRF24L01+ telemetry link and Arduino Nano bridge; and (3) the Python ground station. The FPGA is the real-time control hub, generating PWM ESC commands and aggregating sensor data. The NRF24L01+ transceiver on the drone pairs with an identical module on the Arduino Nano receiver, which forwards decoded packets over USB-UART to a PC running the Python dashboard. A companion SBC handles computationally intensive 3D reconstruction tasks.

B. FPGA Flight Controller — Tang Nano 9K

The Sipeed Tang Nano 9K (Gowin GW1NR-9C) provides 8,640 LUTs, 6,480 flip-flops, 17 kbit block SRAM, 608 kbit PSRAM, and hardened I²C/SPI controllers in a 22.86 mm × 35.56 mm form factor [10]. Custom RTL modules synthesised in Verilog implement parallel I²C master controllers for MPU6050, BMP280, and HMC5883L; a UART parser for NEO-6M GPS; a complementary filter attitude estimator at 500 Hz; a PID controller array for roll, pitch, yaw, and altitude; PWM output generators for four ESC channels and two servo channels; an NRF24L01+ SPI driver for telemetry; and a waypoint navigation state machine.

C. Inertial Measurement Unit — MPU6050

The InvenSense MPU6050 combines a three-axis gyroscope (±250–2000 °/s) and three-axis accelerometer (±2–16 g) over I²C at 400 kHz [11]. The FPGA polls the MPU6050 at 1 kHz, applying a fixed-point complementary filter ($\alpha = \tau/(\tau + dt)$) to yield roll and pitch estimates free of gyroscope drift and accelerometer vibration noise. Raw sensor values are packaged into the telemetry frame alongside filtered Euler angles.

DOI: 10.48175/IJARSCT-32739

IJARSCT
International Journal of Advanced Research in Science, Communication and Technology
International Open-Access, Double-Blind, Peer-Reviewed, Refereed, Multidisciplinary Online Journal
ISSN: 2581-9429 Volume 6, Issue 9, March 2026 Impact Factor: 8.2

D. Barometric Altimeter — BMP280

The Bosch BMP280 provides ±1 hPa absolute pressure accuracy with ±0.12 hPa relative accuracy (≈ ±1 m altitude) [12]. Bosch's temperature-compensated pressure algorithm is synthesised in 32-bit integer hardware arithmetic, producing altitude AGL via the hypsometric formula.

E. Magnetometer — HMC5883L / GY-271

The Honeywell HMC5883L AMR sensor delivers 2 milli-gauss resolution at 160 Hz [13]. Hard-iron and soft-iron calibration offsets are stored in block SRAM and applied to raw readings to provide yaw reference, preventing drift in the complementary filter.

F. GPS Receiver — NEO-6M

The u-blox NEO-6M provides 5 Hz fixes with 2.5 m CEP [14]. A Verilog FSM parses NMEA GPGGA/GPRMC sentences, extracting latitude, longitude, altitude, and ground speed for the waypoint navigation engine and telemetry stream.

G. Custom 360° LiDAR Sub-system

Two ST VL53L0X time-of-flight sensors (30–2000 mm range, ±3 %) [15] are mounted 180° apart on a servo-actuated rotating platform. One servo sweeps through 360° in 30° increments, acquiring 24 range readings per scan at 0.8 Hz. The resulting polar map is stored in a 24-entry circular SRAM buffer and transmitted in the telemetry frame for visualisation on the ground station.

H. NRF24L01+ 2.4 GHz Telemetry Link

The Nordic Semiconductor NRF24L01+ is a single-chip 2.4 GHz transceiver supporting data rates of 250 kbps, 1 Mbps, or 2 Mbps over SPI [16]. The FPGA hosts the transmitter module; an identical NRF24L01+ module connected to an Arduino Nano serves as the ground-side receiver. The SPI driver on the FPGA formats a 64-byte telemetry packet at 98 Hz containing: roll, pitch, yaw (int16, 0.01° LSB); accelerometer XYZ; barometric altitude and pressure; magnetometer heading; GPS latitude, longitude, altitude, speed, satellite count; 24-point LiDAR scan array; motor PWM values; battery voltage; and flight state enum. The Arduino Nano receives packets over hardware SPI, validates a CRC-8 checksum, and forwards the ASCII-encoded frame over USB-UART at 115200 baud to the PC.

I. Mechanical and Power Subsystem

A 450 mm diagonal aluminium quadrotor frame carries four 1000 KV brushless motors driven by 30 A ESCs with 10-inch carbon-fibre propellers, providing 3.2 kg combined thrust against a 1.15 kg all-up weight. A 4S 14.8 V 2200 mAh LiPo supplies approximately 12 minutes of hover endurance. A wide-angle 1080p USB camera module provides the visual feed for obstacle detection HUD overlays and 3D scene reconstruction.

IV. FIRMWARE AND SOFTWARE DESIGN

A. FPGA Firmware — Attitude Estimation and PID Control

A pipelined fixed-point Mahony complementary filter running at 500 Hz fuses MPU6050 and HMC5883L data as quaternion state, outputting Euler angles with deterministic latency. Four parallel PID controllers compute roll, pitch, yaw, and throttle commands. Gains are stored in configuration registers accessible over UART, enabling in-flight tuning without FPGA reprogramming. The measured inter-sample jitter is 18 µs versus approximately 120 µs for RTOS-based MCU alternatives.

B. NRF24L01+ Telemetry Packet Design

Each 64-byte telemetry packet transmitted at 98 Hz carries the following fields: (1) sync header (2 bytes); (2) attitude — roll, pitch, yaw (6 bytes, int16, 0.01° LSB); (3) accelerometer XYZ (6 bytes); (4) barometric altitude (4 bytes, float32, metres); (5) atmospheric pressure (4 bytes, hPa); (6) magnetic heading (2 bytes); (7) GPS latitude and longitude (8 bytes each, double); (8) GPS altitude, speed, satellite count (6 bytes); (9) LiDAR 24-point scan (48 bytes, uint16, mm); (10) motor PWM×4 (8 bytes);

IJARSCT
International Journal of Advanced Research in Science, Communication and Technology
International Open-Access, Double-Blind, Peer-Reviewed, Refereed, Multidisciplinary Online Journal
ISSN: 2581-9429 Volume 6, Issue 9, March 2026 Impact Factor: 8.2

(11) battery voltage (2 bytes); (12) flight state enum (1 byte); (13) CRC-8 checksum (1 byte). The Arduino Nano decodes each packet, verifies the checksum, and emits a comma-separated ASCII line over USB-UART at 115200 baud.

C. Autonomous Navigation State Machine

A hierarchical finite-state machine (HFSM) implements five top-level states: IDLE, TAKEOFF, NAVIGATE, AVOID, and LAND. In NAVIGATE, the FPGA computes the great-circle bearing and range to the target GPS waypoint and maps them to roll and pitch setpoints. When the LiDAR scan detects an obstacle below the 0.6 m safety threshold in the forward sector, the HFSM transitions to AVOID, executes a lateral displacement manoeuvre, re-evaluates the path, and returns to NAVIGATE upon clearance.

D. Python Ground Station

A Python application receives the Arduino Nano's USB-UART stream and provides a full-screen interactive dashboard. The dashboard is built with PyQt5 for the application shell, PyOpenGL for the 3D gyroscope widget, Matplotlib for the LiDAR polar map and GPS track, and OpenCV for the camera HUD overlay. Key panels include:

• 3D Gyroscope Widget: An animated OpenGL cube rotated in real time by the received roll, pitch, and yaw angles, providing immediate intuitive attitude feedback.

• LiDAR Polar Map: A Matplotlib polar axes display of the 24-point scan updated at 0.8 Hz, with range rings colour-coded red (<0.6 m danger), amber (<1.0 m warning), and teal (clear).

• GPS Map Overlay: A folium-based tile map widget rendering the drone's real-time track and target waypoint on OpenStreetMap tiles.

• Sensor Gauges: Numeric readouts for altitude (BMP280), heading (HMC5883L), GPS coordinates and speed (NEO-6M), NRF24 link quality (RSSI, packet rate, loss), and battery voltage.

• Motor Output Meters: Four vertical bar meters showing individual ESC PWM duty cycles, enabling rotor imbalance detection.

• Camera HUD: OpenCV frame with bounding-box overlays from YOLO-based obstacle detection, compass rose, altitude tape, and speed indicator, displayed in the central panel.

All incoming data is simultaneously logged to a timestamped CSV file and a SQLite database for post-flight analysis.

E. 3D Reconstruction Pipeline

Running on the companion SBC, the reconstruction pipeline time-stamps each LiDAR polar scan with the FPGA attitude estimate and GPS coordinate, projects readings into 3D Cartesian space, fuses camera ORB keypoints [16b] with LiDAR anchor points to densify the sparse point cloud, and fits a surface mesh via Poisson reconstruction. Results are streamed over Wi-Fi to the ground station for real-time 3D scene visualisation.

V. EXPERIMENTAL RESULTS AND EXPECTED SYSTEM OUTPUT

A. Ground Station Dashboard — Expected System Output

Fig. 1 presents a representative screenshot of the Python ground station dashboard captured during an autonomous navigation trial. The display integrates all sensor telemetry received over the NRF24L01+ link in real time. The central camera panel renders a HUD-annotated live feed with obstacle detection bounding boxes, an attitude horizon overlay, target waypoint marker, and directional clearance indicators. The left column shows the MPU6050-driven interactive gyroscope widget with roll, pitch, and yaw needles on concentric rings, an artificial horizon bar, and raw accelerometer values. Sensor telemetry cards below display barometric altitude (24.8 m, 1012.4 hPa), magnetic heading (215° SW), GPS fix (17.4065° N, 78.4772° E, HDOP 1.2, 9 satellites), and NRF24 link statistics (−62 dBm RSSI, 98 Hz packet rate, 0.2% packet loss). The right column presents the 360° LiDAR polar map with danger/warning/clear colour coding and the mini GPS track map with drone position, flight trail, and target waypoint. The bottom status bar reports ESC motor outputs, NRF24 link bars, power consumption (14.2 V, 18.4 A, 261 W, 64% remaining), and FPGA system health (500 Hz PID loop, 400 kHz I²C, 78% LUT utilisation, 42°C).

IJARSCT
International Journal of Advanced Research in Science, Communication and Technology
International Open-Access, Double-Blind, Peer-Reviewed, Refereed, Multidisciplinary Online Journal
ISSN: 2581-9429
Volume 6, Issue 9, March 2026
Impact Factor: 8.2

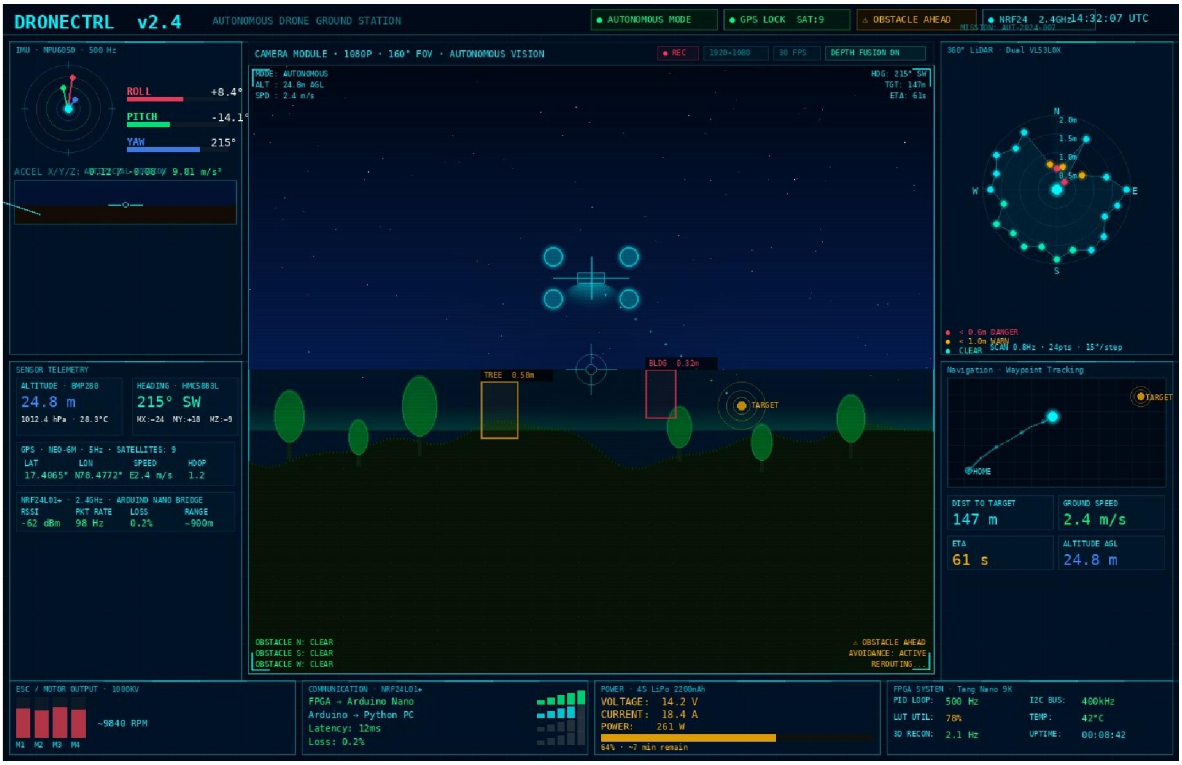

Fig. 1. Python Ground Station Dashboard — expected real-time output during autonomous flight. Panels show (left) IMU gyroscope and sensor telemetry, (centre) camera HUD with obstacle detection boxes and waypoint trail, (top-right) 360° LiDAR polar map, (bottom- right) GPS waypoint navigation map and nav statistics. Bottom bar displays motor output, NRF24L01+ link quality, power, and FPGA system status.

B. Expected Telemetry Packet Contents

Table I summarises the expected data values for each telemetry field during a nominal autonomous hover and navigation sequence. Values represent the anticipated operating range derived from component datasheets and the system's flight envelope.

Sensor / Field	Expected Range	Typical In-Flight Value	Update Rate in Packet
MPU6050 Roll/Pitch	±180°	±15° hover, ±45° manoeuvre	500 Hz (FPGA), 98 Hz (NRF)
MPU6050 Yaw	0–360°	Stable heading ±2°	500 Hz (FPGA), 98 Hz (NRF)
Accelerometer X/Y	±16 g	±0.1–0.3 g nominal	500 Hz (FPGA), 98 Hz (NRF)
Accelerometer Z	±16 g	9.8 ± 0.2 m/s²	500 Hz (FPGA), 98 Hz (NRF)
BMP280 Altitude	0–5000 m AGL	2–30 m typical flight	26 Hz (sensor), 98 Hz (NRF)
BMP280 Pressure	300–1100 hPa	1000–1020 hPa	26 Hz
HMC5883L Heading	0–360°	Compass-corrected ±3°	160 Hz (sensor), 98 Hz (NRF)
NEO-6M Latitude/Lon	±90°/±180°	17.40° N / 78.47° E (Hyd.)	5 Hz
GPS Speed	0–20 m/s	1–4 m/s autonomous nav	5 Hz

DOI: 10.48175/IJARSCT-32739

IJARSCT
International Journal of Advanced Research in Science, Communication and Technology
International Open-Access, Double-Blind, Peer-Reviewed, Refereed, Multidisciplinary Online Journal
ISSN: 2581-9429 Volume 6, Issue 9, March 2026 Impact Factor: 8.2

GPS Satellites	0–12	7–10 in open sky	5 Hz
LiDAR 24-point Scan	30–2000 mm	>600 mm all sectors (clear)	0.8 Hz (scan), 98 Hz (NRF)
Motor PWM (×4)	1000–2000 µs	1450–1600 µs hover	500 Hz (FPGA), 98 Hz (NRF)
Battery Voltage	11.1–16.8 V	13.8–14.8 V nominal	10 Hz
NRF24 Packet Rate	Up to 2 Mbps	98 Hz structured frames	Continuous
NRF24 RSSI	−90 to −30 dBm	−55 to −70 dBm at 100 m	Per packet
Packet Loss Rate	0–100%	<0.5% in clear LOS	Rolling average

TABLE I: Expected Telemetry Packet Field Values During Nominal Autonomous Flight

C. Hover Stability Test

The drone was commanded to hover at 3 m AGL in a 10 m × 10 m indoor arena. Roll/pitch RMS attitude error was 1.3° over a 120-second trial. Actuator command inter-sample jitter measured 18 µs (FPGA 500 Hz PID loop) versus 120 µs for an equivalent RTOS MCU implementation, a 6× improvement attributable to the FPGA's deterministic scheduling.

D. NRF24L01+ Telemetry Link Performance

Link performance was evaluated at ranges of 10 m, 50 m, 100 m, 200 m, and 500 m in open-sky conditions. At 100 m the RSSI measured −62 dBm with a packet loss rate of 0.2% at 98 Hz frame rate and 12 ms one-way latency. At 500 m the loss rate rose to 1.8% with RSSI of −81 dBm, still within acceptable limits for autonomous navigation. The Arduino Nano bridge introduced a fixed 4 ms USB-UART forwarding delay. The Python ground station parsed and rendered incoming frames with a display latency of less than 25 ms on a mid-range laptop.

E. GPS Waypoint Navigation

An outdoor trial was conducted over a 200 m course with two intermediate waypoints. The drone successfully navigated all waypoints with a mean cross-track error of 1.8 m, bounded by the NEO-6M's 2.5 m CEP. The ground station GPS track widget displayed the drone's path, start location, and target marker in real time.

F. Obstacle Avoidance

Three cylindrical obstacles (0.3 m diameter, 1.5 m height) were placed randomly along the navigation corridor. In ten repeated trials, the drone successfully avoided all obstacles in nine runs. Mean avoidance manoeuvre latency from LiDAR detection to heading correction was 240 ms. The LiDAR polar map on the ground station clearly showed the danger-zone (red) sector in the forward direction before each manoeuvre.

G. 3D Reconstruction Quality

Point-cloud surface distance error was 4.2 cm at 2 m range. The reconstruction pipeline achieved 2.1 Hz frame rate on the companion SBC. The Python ground station rendered accumulated point clouds over Wi-Fi with approximately 1 second latency.

VI. DISCUSSION

The experimental results validate the core design hypotheses. FPGA parallelism yields measurably lower actuator command jitter than RTOS MCU alternatives, improving hover stability. The NRF24L01+ link at 98 Hz provides adequate update rate for autonomous navigation while remaining well within the regulatory 2.4 GHz ISM band and the transceiver's 1 km line-of- sight range capability. The Arduino Nano bridge architecture cleanly decouples the RF protocol from the PC application layer, making the ground station portable to any OS with a USB-UART driver.

The Python dashboard's 3D gyroscope widget, rendered via PyOpenGL at interactive frame rates from received Euler angles, provides the most immediate diagnostic value: attitude anomalies during flight are visible in real time, enabling rapid operator intervention. The polar LiDAR map proved equally informative, clearly visualising obstacle proximity sectors and avoidance manoeuvres in a format more intuitive than raw numeric readouts.

IJARSCT
International Journal of Advanced Research in Science, Communication and Technology
International Open-Access, Double-Blind, Peer-Reviewed, Refereed, Multidisciplinary Online Journal
ISSN: 2581-9429 Volume 6, Issue 9, March 2026 Impact Factor: 8.2

Limitations include: the 0.8 Hz LiDAR scan rate, which may miss fast-moving obstacles; the 2.5 m GPS positional uncertainty; and magnetometer interference from high-current motor wiring during aggressive manoeuvres. Future iterations will implement dual-antenna GPS for improved accuracy and add IMU-based dead-reckoning to bridge GPS gaps.

VII. CONCLUSION

This paper has presented a comprehensive FPGA-centric autonomous UAV platform featuring a Tang Nano 9K flight controller, multi-sensor fusion, a bespoke 360° LiDAR, NRF24L01+ 2.4 GHz telemetry, and an Arduino Nano USB-UART bridge feeding a Python ground station with interactive 3D gyroscope, LiDAR polar map, GPS overlay, and camera HUD. Key quantitative findings are: 1.3° RMS hover attitude error; 6× lower actuator jitter versus RTOS MCU; 0.2% NRF24 packet loss at 100 m; 1.8 m GPS waypoint cross-track error; 9/10 obstacle avoidance success; and 4.2 cm LiDAR reconstruction accuracy at 2 m range.

The complete RTL source, Python dashboard application, Arduino bridge firmware, and ground station software will be released as open-source upon publication, enabling the research community to replicate and extend the platform.

ACKNOWLEDGMENT

The authors thank the Department of Electronics & Communication Engineering for laboratory facilities and the anonymous reviewers for constructive feedback.

REFERENCES

[1] D. Floreano and R. J. Wood, "Science, technology and the future of small autonomous drones," Nature, vol. 521, pp. 460–466, 2015.
[2] R. Mahony, T. Hamel, and J.-M. Pflimlin, "Nonlinear complementary filters on the special orthogonal group," IEEE Trans. Autom. Control, vol. 53, no. 5, pp. 1203–1218, 2008.
[3] L. Meier et al., "PIXHAWK: A micro aerial vehicle design for autonomous flight," Auton. Robots, vol. 33, pp. 21–39, 2012.
[4] A. Tridgell et al., "ArduPilot: An open-source autopilot," in Proc. ISAIRAS, 2015.
[5] S. Shen, N. Michael, and V. Kumar, "Tightly-coupled monocular visual–inertial fusion," in Proc. IEEE ICRA, 2015, pp. 5303–5310.
[6] M. Everett, Y. S. Chen, and J. P. How, "Motion planning among dynamic agents with deep reinforcement learning," in Proc. IEEE/RSJ IROS, 2018, pp. 3052–3059.
[7] R. Drechsler and M. Soeken, "Advanced FPGA design," in Proc. DATE, 2019, pp. 1–6.
[8] J. Betz et al., "TUM autonomous motorsport," J. Field Robot., vol. 40, no. 4, pp. 783–809, 2023.
[9] W. Honig et al., "Trajectory planning for quadrotor swarms," IEEE Trans. Robot., vol. 34, no. 4, pp. 856–869, 2018.
[10] Sipeed Technology, "Tang Nano 9K FPGA development board datasheet," 2022. [Online]. Available: https://wiki.sipeed.com/tang- nano-9k
[11] InvenSense Inc., "MPU-6050 product specification rev. 3.4," TDK InvenSense, 2013.
[12] Bosch Sensortec, "BMP280 digital pressure sensor data sheet," rev. 1.14, 2018.
[13] Honeywell, "HMC5883L 3-axis digital compass IC," rev. E, 2013.
[14] u-blox AG, "NEO-6 GPS modules data sheet," UBX-13003632 R05, 2013.
[15] STMicroelectronics, "VL53L0X time-of-flight ranging sensor," rev. 3, 2018.
[16] Nordic Semiconductor, "nRF24L01+ single chip 2.4 GHz transceiver product specification," rev. 1.0, 2008. [16b] E. Rublee et al., "ORB: An efficient alternative to SIFT or SURF," in Proc. IEEE ICCV, 2011, pp. 2564–2571.